ΕΡΓΟΔΟΤΗΣ

Αρχή Λιμένων Κύπρου

ΕΡΓΟ

ΕΠΙΚΑΙΡΟΠΟΙΗΜΕΝΗ ΜΕΛΕΤΗ
ΕΚΤΙΜΗΣΗΣ ΕΠΙΠΤΩΣΕΩΝ ΣΤΟ ΠΕΡΙΒΑΛΛΟΝ (ΜΕΕΠ)
ΓΙΑ ΤΗΝ ΕΠΕΚΤΑΣΗ ΤΟΥ
ΛΙΜΕΝΑ ΛΕΜΕΣΟΥ – ΤΕΡΜΑΤΙΚΟ 2 (ΒΑΣΙΛΙΚΟ)

ΤΙΤΛΟΣ ΕΓΓΡΑΦΟΥ

ΑΚΤΟΜΗΧΑΝΙΚΗ ΜΕΛΕΤΗ

ΑΡ. ΕΓΓΡΑΦΟΥ

1184-A2-E2

ΗΜΕΡ. ΕΓΓΡΑΦΟΥ

20 Δεκεμβρίου 2023

ΣΥΜΒΟΥΛΟΙ

TOUMAZIS

Dion. Toumazis & Associates L.L.C.

Ρωμανού 4, 1070 Λευκωσία
Τηλ. 22374027, Φαξ. 22374933
e-mail: mail@diontoumazis.com
www.diontoumazis.com

Ρογκάν & Συνεργάτες Α.Ε

Χατζηγιάννη Μέξη 5, 11528 Αθήνα, Ελλάδα
Τηλ. +30-210-7782405
e-mail: rogan@otenet.gr
www.roganassoc.gr

Σύνταξη	Γεώργιος Φώτης 
Έλεγχος	Δρ. Χρήστος Σολομωνίδης 

CONTENTS

LIST OF FIGURES

LIST OF TABLES

2	20/12/2023	Τελική Υποβολή	Γεώργιος Φώτης	Δρ. Χρήστος Σολομωνίδης
1	18/12/2023	Υποβολή	Γεώργιος Φώτης	Δρ. Χρήστος Σολομωνίδης
Έκδοση	Ημερ.	Περιγραφή	Ετοιμασία	Έλεγχος

EXECUTIVE SUMMARY

Αντικείμενο της παρούσας μελέτης αποτελεί η προσομοίωση των παράκτιων διεργασιών που προκαλούν αλλαγές στην παράκτια υδραυλική και γεωμορφολογία (δηλαδή των υψών κύματος, κυματογενών ρευμάτων, ρυθμών μεταφοράς ιζήματος & μεταβολές της στάθμης του πυθμένα) μεταξύ της υφιστάμενης κατάστασης (Do Nothing) και της προτεινόμενης γενικής διάταξης (W1).

Αρχικά πραγματοποιήθηκε ανάλυση του κυματικού κλίματος της περιοχής (Κεφάλαιο 3), από όπου προέκυψε ότι οι επικρατέστερες διευθύνσεις είναι η ΝΝΔ και η ΔΝΔ με ετήσιες συχνότητες εμφάνισης 52.66% και 33.88% αντίστοιχα. Συνολικά προσομοιώθηκαν δέκα (10) κυματικές περιπτώσεις, δύο (2) από κάθε τομέα προέλευσης, όπως παρουσιάζονται στον παρακάτω πίνακα (Table 3-5).

Για την διερεύνηση των κυρίαρχων ακτομηχανικών διεργασιών που επικρατούν στην περιοχή μελέτης, αρχικά πραγματοποιήθηκε αριθμητική προσομοίωση της υφιστάμενης κατάστασης. Συγκεκριμένα η προσομοίωση έγινε εφαρμόζοντας την αλληλουχία των μοντέλων της εταιρίας DHI (φασματικό, υδροδυναμικό και στερεομεταφοράς). Από τα αποτελέσματα των προσομοιώσεων παρατηρούνται εναλλασσόμενες τάσεις απόθεσης και διάβρωσης κατά μήκος της ακτής ανατολικά του λιμένα. Στη δυτική πλευρά του λιμένα και πιο συγκεκριμένα στη ρίζα του προσήνεμου κυματοθραύστη παρατηρούνται κυρίαρχες τάσεις απόθεσης και περιορισμένες. Σημειώνεται ότι η συγκεκριμένη περιοχή είναι μη-διαβρώσιμη λόγω της ύπαρξης θωράκισης του παραλιακού μετώπου. Συνολικά, οι τάσεις προσάμμωσης είναι εμφανείς στην προσήνεμη πλευρά των υφιστάμενων κατασκευών.

Τα βασικά συμπεράσματα που προέκυψαν από την προσομοίωση της Γενικής Διάταξης W1 συγκριτικά με αυτή της DN συνοψίζονται παρακάτω:

- Η επέκταση του προσήνεμου κυματοθραύστη προσφέρει σημαντική προστασία στην περιοχή ανατολικά του λιμανιού για κύματα που προσπίπτουν από ΔΝΔ, ΝΝΔ και Ν κατευθύνσεις
- Παρατηρείται ότι οι κυρίαρχες τάσεις που προκύπτουν από την ετήσια ενσωμάτωση όλων των γεγονότων είναι παρόμοιες με αυτές που προκύπτουν από τα Νότιο-Νοτιοδυτικά Κύματα, όπως και στην περίπτωση DN.
- Στην ακτή δυτικά του λιμένα, και πιο συγκεκριμένα στη ρίζα του προσήνεμου κυματοθραύστη, οι τάσεις απόθεσης εντείνονται σε σύγκριση με το σενάριο DN
- Στην ανατολική πλευρά του λιμανιού, η περιοχή που επηρεάζεται από τα έργα εκτείνεται από τη ρίζα του νέου υπήνεμου κυματοθραύστη μέχρι 600 μέτρα περίπου προς τα ανατολικά.
- Η γενική τάση στην περιοχή επιρροής είναι να υπάρχουν πιο ήρεμες περιοχές, με μειωμένες τάσεις διάβρωσης συγκριτικά με την υφιστάμενη κατάσταση - σενάριο DN

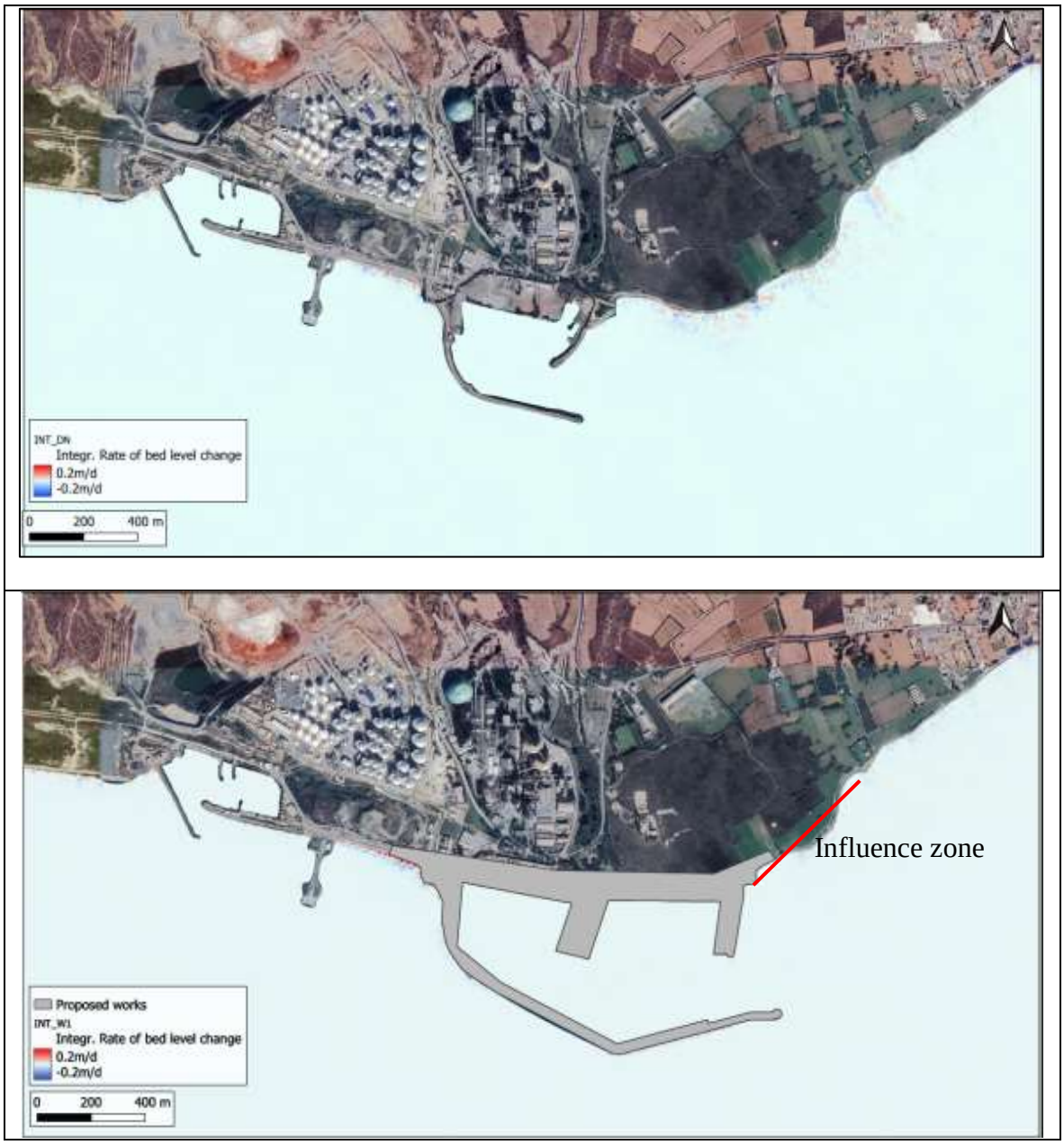

Το συνολικό συμπέρασμα είναι ότι η επέκταση του λιμένα δεν θα επηρεάσει αρνητικά την εξέλιξη της παράκτιας γεωμορφολογίας στη ανατολική πλευρά του υπάρχοντος λιμένα, ενώ οι ελαφρώς επαυξημένες τάσεις απόθεσης στα δυτικά, συγκριτικά με την υφιστάμενη κατάσταση, δεν αξιολογούνται ως σημαντικές και δεν απαιτούν δράσεις μετριασμού.

1. INTRODUCTION

An investigation of coastal impacts is carried out, by means of numerical simulation, for the proposed expansion of Limassol Port – Terminal 2 (Vassilikos).

The present study is prepared by the Joint Venture of the Consulting Engineering Firms "ROGAN & Associates S.A. and Dion. Toumazis & Associates" for the Cyprus Ports Authority.

Breakwaters can affect local wave climate, currents and sediment transport processes and can cause changes in the configuration of the adjacent shoreline.

The scope of the preset study is to simulate the changes in the coastal hydraulics (namely wave heights, wave-induced currents, sediment transport rates, sea bed level changes) between the ones in the existing (Do Nothing) situation and the proposed general arrangement (W1) and assess the potential coastal impacts associated with these changes.

2. DESCRIPTION OF EXISTING PORT INFRASTRUCTURE AND FUTURE EXPANSION

2.1. Existing Port Infrastructure

Vassilikos Port is located at the eastern side of Vassiliko Bay (see Figure 2-1). It is currently operated by Vassiliko Cement Works under a concession agreement with the Cyprus Ports Authority for a period of 50 years, i.e. until 2032. The port is capable to handle dry and liquid bulk cargos.

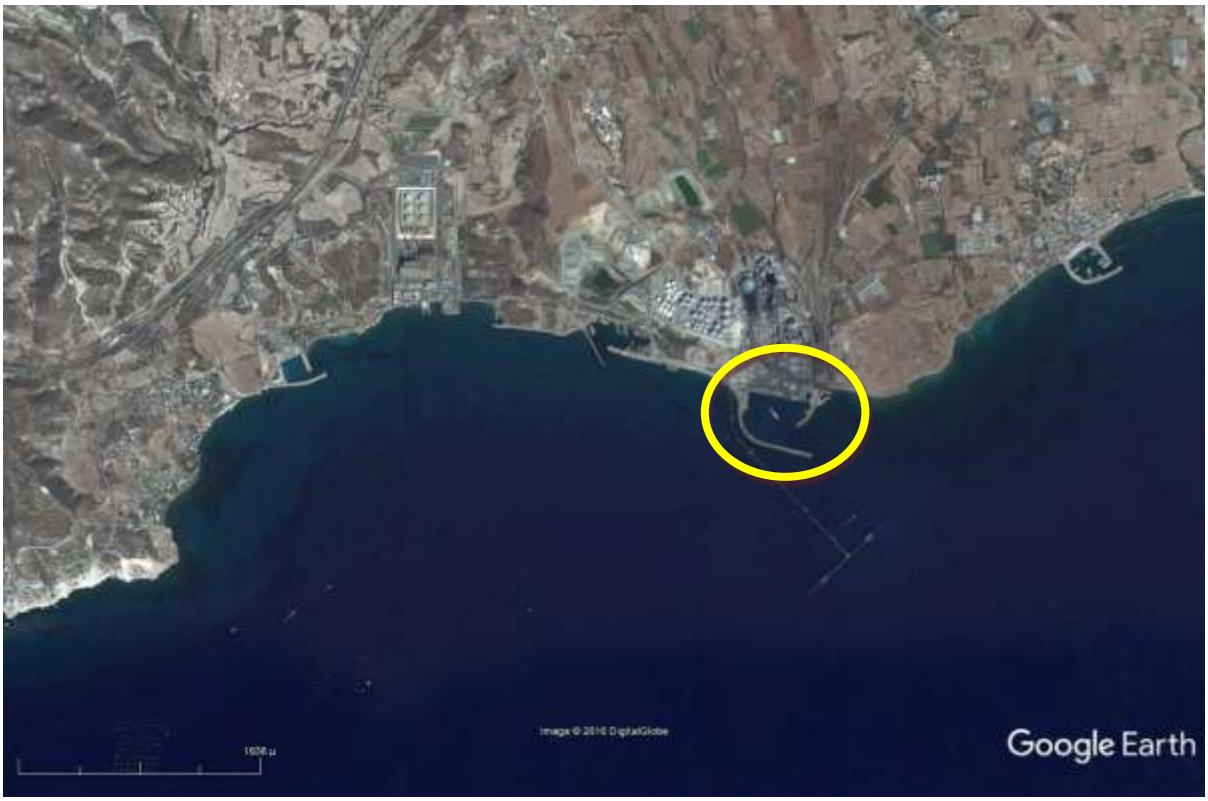

Figure 2-1. Location of Vassilikos Port (indicated with yellow circle).

The port is protected by two breakwaters, the southern (windward) and the eastern (leeward). The port entrance is orientated eastwards (see Figure 2-2). There are two main quays, the northern of 360m length and the western of 125m. It has a turning circle of 280m diameter, and the water depth is about 9m (below CD).

Figure 2-2. Existing Port Infrastructure of Vassiliko.

2.2. Future Expansion

The reason for the proposed expansion of the port is the provision of enlarged marine infrastructure in order to meet future demands relating to dry bulk cargos as well as to form a potential supply base to support offshore drilling operations envisaged mainly in the area of Cyprus, Israel and Egypt.

The main works comprise the following (see Figure 2-3):

- Removal of the last 400m of the existing windward breakwater and 1240m extension
- Construction of a new 275m long leeward breakwater
- Construction of a 230m long x 125m wide pier at the location of the existing leeward breakwater
- Extension of coastal quay westward of the existing port basin 115m long / -9m deep.
- Extension of the quay to the north of the existing port basin 50m long / -9m deep
- Construction of a new quaywall north of the new port basin 385m long / -15m deep.
- Construction of a new quaywall east of the new port basin 195m long /-15m deep.
- Construction of a new quaywall along the inner side of the windward breakwater 1035m long / variable depth between -9m, -13m and -15m.
- Dredging of the new port basin at -15m CD
- Dredging the area between the new and the existing port basin at -13m CD

- Dredging of the new entrance channel at -16.5m CD

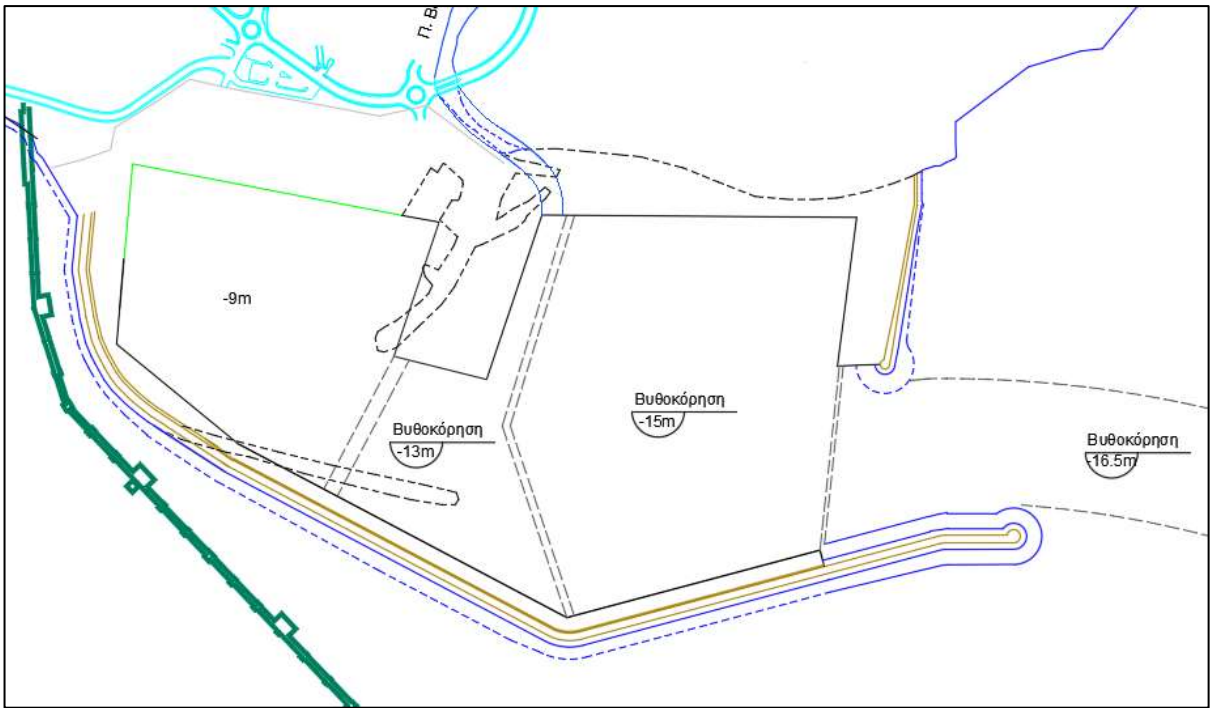

Figure 2-3. Proposed works

2.3. Adjacent shorelines

The adjacent shorelines eastern and western of Limassol Port Terminal 2 (Vassiliko) are depicted in the following figure.

Figure 2-4. Adjacent shorelines to Limassol Port Terminal 2 (Vassiliko).

At the west side of the port, there is a coastline of about 370m length, extending from the windward breakwater's root up to a the "Skyra Vassa" pier (see Figure 2-5).

At the east side of the port there is a coastline of nearly 2km length, extending from the leeward breakwater's root up to the Zygi fishing shelter (see Figure 2-6).

Figure 2-5. Adjacent coast at the west side of Vassiliko's Port.

Figure 2-6. Adjacent coast at the east side of Vassiliko's Port up to Marina Zygi.

2.4. Historical Evolution of Shoreline Morphology

Historical information, regarding the evolution of shoreline morphology, is of great importance in identifying accretion or erosion areas, temporal variations in bathymetry, information on existing structures, pre-existing coastal features, etc. For example accretion and erosion may be assessed by comparison of geo-referenced images/maps taken at distinct years of the period of interest. Such information is available, for the specific study area, through the online platform http://eservices.dls.moi.gov.cy as published by the Department of Lands and Survey - Ministry of Interior (Republic of Cyprus).

The present study uses the information provided by the interactive maps (see Figure 2-7), indicating the shoreline morphology for the following years 1963, 1993, 2003 and 2008. Furthermore, erosion and accretion areas are highlighted with pink and light blue colors respectively.

Inspection of these figures indicates erosion trends along the coastline from 1963 up to 2008 at the east side of the port.

Figure 2-7. Historical evolution of shoreline morphology. Pink color indicates erosion areas while light blue indicates accretion areas (natural or artificial) (Department of Lands and Survey - Ministry of Interior).

Figure 2-8. Erosion and accretion areas at the east side coast of the port (Department of Lands and Survey - Ministry of Interior). Pink color indicates erosion areas while light blue indicates accretion areas

3. WAVE CLIMATE

The present study uses wave data in the study area, as presented in previous reports:

- Annual wave roses (at depth -15m, in the vicinity of Vassilikos) as illustrated (see Figure 3-1) in the study of HR Wallingford (2006). The wave characteristics are given in Table 3-1.
- Offshore wave climate (see Figure 3-2), South of Cyprus, as obtained from ship observations from 1961 to 1980. This study was carried out by Delft Hydraulics (1990, 1991).

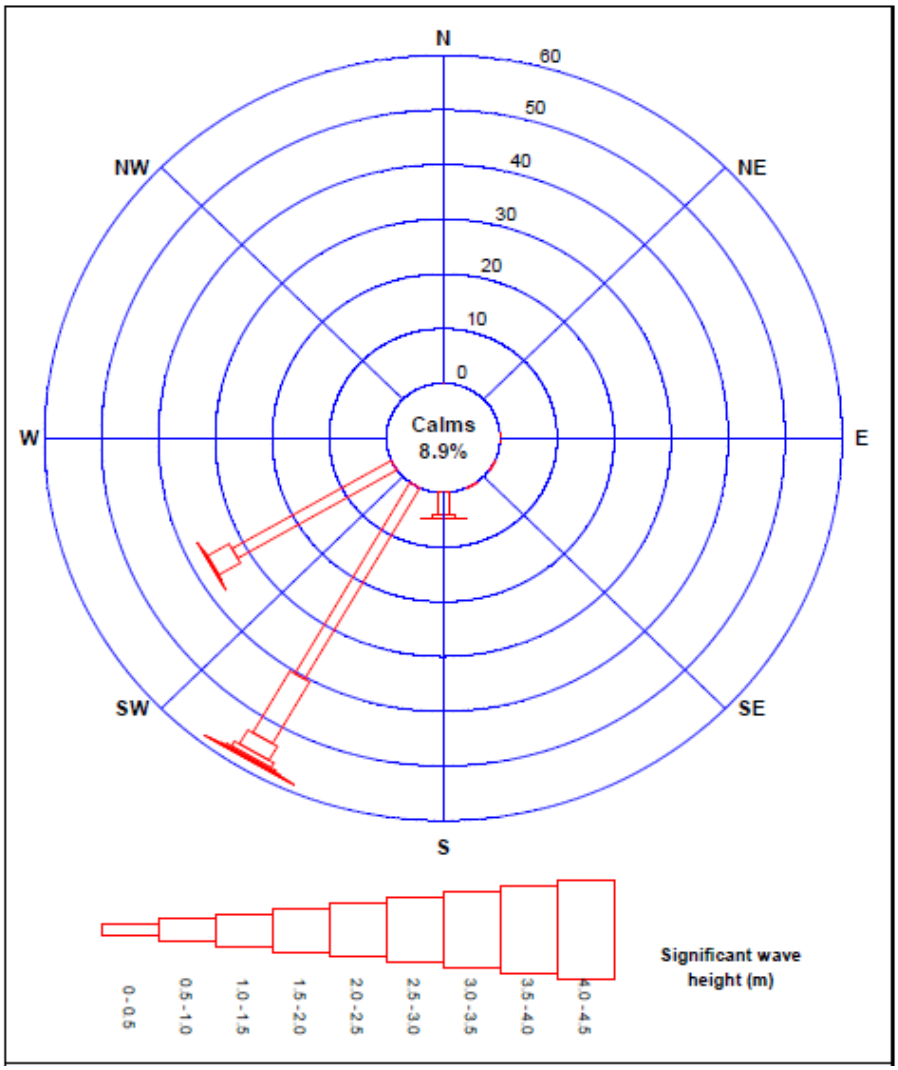

Figure 3-1. Inshore annual wave rose at 15m depth (HR Wallingford, 2006).

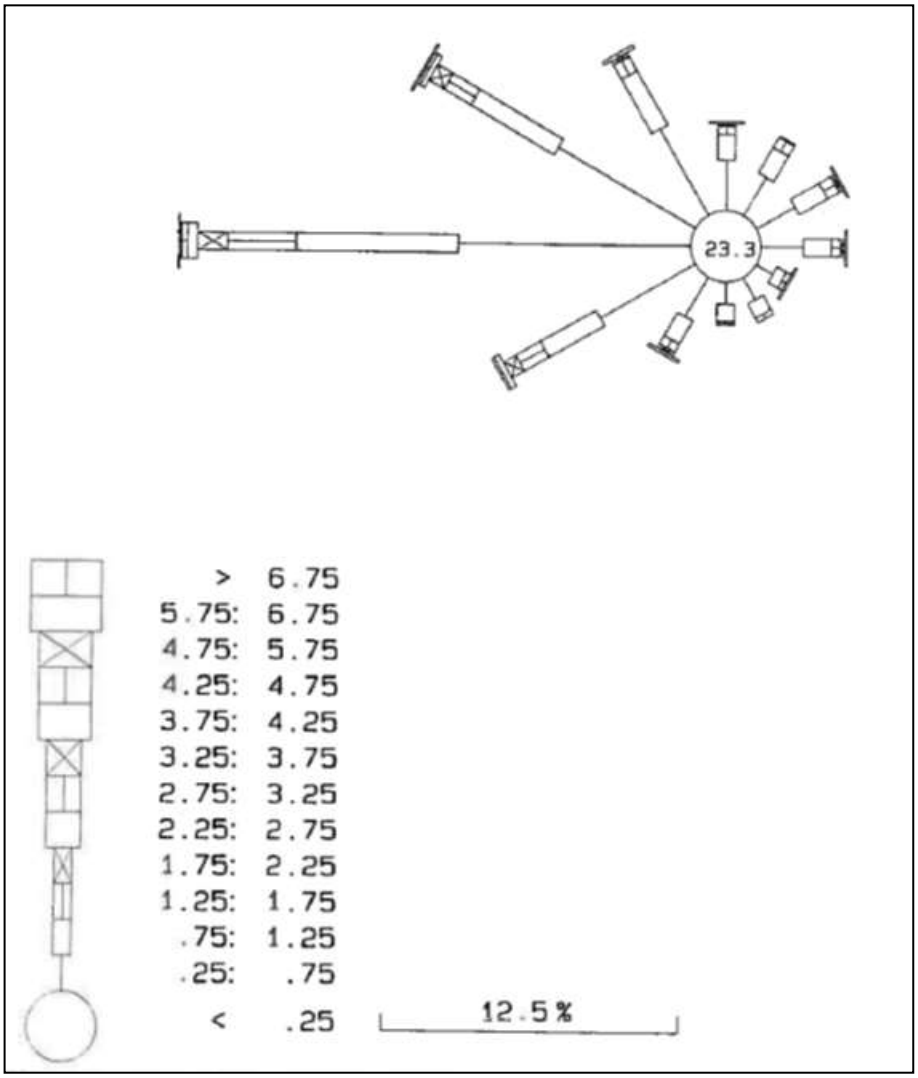

Figure 3-2. Annual offshore wave rose, south of Cyprus (Delft Hydraulics, 1990, 1991).

Table 3-1. Wave characteristics at 15m depth as extracted from wave roses (HR Wallingford, 2006).

S (N180°)			SSW (N210°)			WSW (N240°)		
f (%)	Hs (m)	Tp (sec)	f (%)	Hs (m)	Tp (sec)	f (%)	Hs (m)	Tp (sec)
3.83	0.5	3.18	36.44	0.5	3.18	30.06	0.5	3.18
0.55	1	4.50	12.03	1	4.50	3.64	1	4.50
			2.73	1.5	5.51			
0.18	2	6.36	1.09	2	6.36			
			0.18	2.5	7.12	0.18	2.5	7.12
			0.18	4.5	9.55			

The offshore wave climate, as provided by the second study, was transferred to nearshore (at depth 15m) by implementing a highly accurate wave propagation model, **MIKE21 S**pectral **W**aves module (DHI, 2016), simulating wave transformation processes (i.e. refraction, shoaling, wave breaking, etc) for SSE and ESE incoming wave directions. The wave characteristics are given in Table 3-2.

Table 3-2. Wave characteristics at 15m depth, as calculated by numerical modeling, by taking as input the offshore wave rose by Delft Hydraulics (1990, 1991).

SSE (N150°)						ESE (N120°)					
offshore			nearshore			offshore			nearshore		
f (%)	Hs (m)	Tp (sec)	Hs (m)	Tp (sec)	Dir (oN)	f (%)	Hs (m)	Tp (sec)	Hs (m)	Tp (sec)	Dir (oN)
0.81	0.5	4.95	0.49	4.95	150.30	1.04	0.5	4.95	0.48	4.95	120.60
0.45	1	5.37	0.95	5.37	150.70	0.68	1	5.37	0.94	5.37	121.20
0.22	1.5	6	1.37	6	151.5	0.21	1.5	6	1.33	6	122.4
0.07	2	7.03	1.72	7.03	153.00	0.03	2	7.03	1.58	7.03	124.7
0.03	2.5	9.86	1.93	9.86	156.00	0.04	2.5	9.86	1.39	9.86	128.90

The most conservative approach is adopted in this study. For directions S, SSW and WSW, the incident wave climate is obtained from HR Wallingford's study, whilst wave climate incident from SSE and ESE is obtained from Delft's study. Table 3-3 presents the nearshore wave climate used as input to the numerical model.

Table 3-3. Adopted wave data at 15m depth, serving as input to the numerical model.

S (N180o)				SSW (N210o)				WSW (N240o)				SSE (N150o)				ESE (N120o)			
A/A	f (%)	Hs (m)	Tp (sec)	A/A	f (%)	Hs (m)	Tp (sec)	A/A	f (%)	Hs (m)	Tp (sec)	A/A	f (%)	Hs (m)	Tp (sec)	A/A	f (%)	Hs (m)	Tp (sec)
1	3.83	0.5	3.18	4	36.44	0.5	3.18	10	30.06	0.5	3.18		0.81	0.5	4.95		1.04	0.5	4.95
2	0.55	1	4.50	5	12.03	1	4.50	11	3.64	1	4.50	13	0.45	1	5.37	17	0.68	1	5.37
				6	2.73	1.5	5.51					14	0.22	1.5	6.00	18	0.21	1.5	6.00
3	0.18	2	6.36	7	1.09	2	6.36					15	0.07	2	7.03	19	0.03	2	7.03
				8	0.18	2.5	7.12	12	0.18	2.5	7.12	16	0.03	2.5	9.86	20	0.04	2.5	9.86
				9	0.18	4.5	9.55												
SUM	4.56				52.66				33.88				1.58				2.00		
																			94.68

The numerical simulation of sediment transport was performed using the Equivalent Wave Climate approach. The methodology followed for each direction of interest is as follows:

First, the representative wave period Te is calculated using the following relation:

$$T_e = \frac{\sum T_i f_i}{f}$$

Where f, is the annual frequency of occurrence of the equivalent wave:

$$f = \sum fi$$

Next, the equivalent wave height He is calculated using the Borah και Balloffet (1985), relation:

$$H_e^2 T_e = \frac{\sum H_i^2 T_i f_i}{f}$$

Where, Hi, Ti, fi, the wave heights, wave periods and frequency of occurrence of the waves that correspond to each direction.

Table 3-4: Calculation of Equivalent wave climate

Direction	m_{wdir} (deg)	H_s(m)	T_p(s)	f (%)	f_{tot} (%)	Hi^2	Te (s)	He (m)	Fe (%)
S	187.5	0.5	3.53	3.83		0.25	**3.85**	**0.80**	**4.560**
		1	5.00	0.55		1			
		2	7.07	0.18		4			
					4.56				
SSW	210	0.5	3.18	36.44		0.25	**3.70**	**0.98**	**52.650**
		1	4.5	12.03		1			
		1.5	5.51	2.73		2.25			
		2	6.36	1.09	52.65	4			
		2.5	7.12	0.18		6.25			
		4.5	9.55	0.18		20.25			
WSW	240	0.5	3.18	30.06		0.25	**3.34**	**0.65**	**33.880**
		1	4.5	3.64		1			
		2.5	7.12	0.18		6.25			
					33.88				
SSE	150	0.5	4.95	0.81		0.25	**5.57**	**1.09**	**1.580**
		1	5.97	0.45		1			
		1.5	6	0.22		2.25			
		2	7.03	0.07	1.58	4			
		2.5	9.86	0.03		6.25			
ESE	120	0.5	4.95	1.04		0.25	**5.33**	**1.02**	**2.000**
		1	5.37	0.68		1			
		1.5	6	0.21		2.25			
		2	7.03	0.03	2	4			
		2.5	9.86	0.04		6.25			

Two (2) wave cases were simulated for each direction of interest:

1. The equivalent wave, as calculated using the Borah και Balloffet (1985) relation (Table 3-4)
2. The highest wave

In total, **10 wave cases** were simulated for each of the alternative layouts (i.e. DN, W1). The wave cases simulated are given in the table below (Table 3-5):

Table 3-5: Wave cases

Direction	m_{wdir} (deg)	He (m)	Te (s)
S	187.5	**0.80**	**3.85**
		2.00	**7.07**
SSW	210	**0.98**	**3.70**
		4.50	**9.55**
WSW	240	**0.65**	**3.34**
		2.50	**7.12**
SSE	150	**1.09**	**5.57**
		2.50	**9.86**
ESE	120	**1.02**	**5.33**
		2.50	**9.86**

4. METHODOLOGY APPLIED AND SCIENTIFIC BACKGROUND OF NUMERICAL MODELS

4.1. Methodology Applied

The methodology adopted is as follows:

1. Determination of three-dimensional distributions of offshore (or at specific depth in intermediate waters) wave characteristics (wave height, period and direction).
2. The bathymetry of the study area is constructed using a flexible mesh with nodes and elements, including the port and the adjacent shorelines.
3. The offshore wave climate and the bathymetry serve as input in the numerical model **MIKE21 SW**, for simulating wave propagation, taking into account all the dominant wave transformation phenomena such as refraction, shoaling and breaking.
4. The radiation stresses, as calculated from the previous step, are given as an input to the hydrodynamic module **MIKE21 FM-HD**, simulating the wave generated currents all over the nearshore field.
5. Simulation of sediment transport field with **MIKE21 FM-ST** is then possible, since the wave and hydrodynamic fields are known. Steps 3, 4 and 5 are applied iteratively for each incoming wave scenario examined.
6. Finally, an annual integration of all incoming wave scenarios is carried out to calculate an annual mean rate of bed level change.

The above procedure is applied firstly for simulating the current situation (Do Nothing scenario, **DN** hereafter) and subsequently, for all the alternative scenarios under investigation (i.e. W1), with different proposed works.

The previous steps are summarized in the following flow chart.

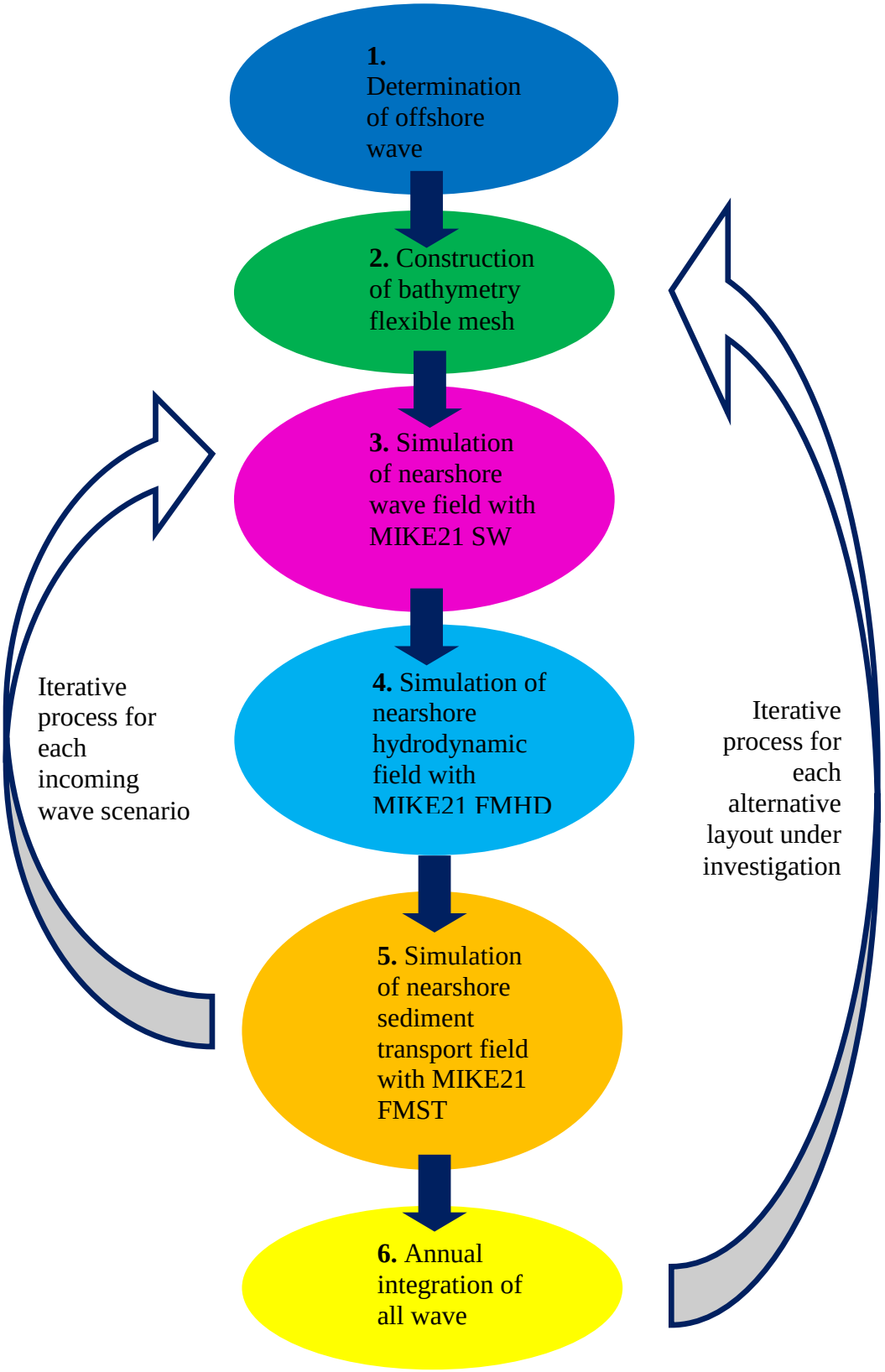
1. Determination of offshore wave
2. Construction of bathymetry flexible mesh
3. Simulation of nearshore wave field with MIKE21 SW
4. Simulation of nearshore hydrodynamic field with MIKE21 FMHD
5. Simulation of nearshore sediment transport field with MIKE21 FMST
6. Annual integration of all wave
Iterative process for each incoming wave scenario
Iterative process for each alternative layout under investigation

4.2. Scientific Background of Numerical Models

4.2.1. MIKE21 Spectral Waves Model

Introduction

As mentioned above, the present study implements the MIKE21 **S**pectral **W**aves model (DHI, 2016) to simulate the wave propagation from offshore to the entrance of the port. MIKE 21 **SW** includes a new generation spectral wind-wave model based on unstructured meshes. The model simulates the growth, decay and transformation of wind-generated waves and swell in offshore and coastal areas. MIKE 21 SW includes the following physical phenomena:

- ✓ Wave growth by action of wind
- ✓ Non-linear wave-wave interaction
- ✓ Dissipation due to white-capping
- ✓ Dissipation due to bottom friction
- ✓ Dissipation due to depth-induced wave breaking
- ✓ Refraction and shoaling due to depth variations
- ✓ Wave-current interaction
- ✓ Effect of time-varying water depth and flooding and drying

Application Areas

MIKE21 SW is used for the assesment of wave climates in offshore and coastal areas – in hindcast and forecast mode. A major aplication area is the design of offshore, coastal and port structures where accurate assessment of wave loads is of utmost importance to the safe and economic design of these structures.

Measured data is often not available during periods long enough to allow for the establishment of sufficiently accurate estimates of extreme sea states. In this case, the measured data can then be supplemented with hindcast data thorugh the simulation of wave conditiions during historical storms using MIKE21 SW.

MIKE21 SW is particularly applicable for simultaneous wave prediction and analysis on regional scale and local scale. Coarse spatial and temoral resolution is used for the regional part of the mesh and a high-resolution boundary- and depth adaptive mesh is describing the shallow water environment at the coastline.

MIKE21 SW is also used in connection with the calculation of the sediment transport, which for a large part is determined by wave conditions and associated wave-induced currents. The wave-induced current is generated by the gradients in radiation stresses that occur in the surf zone. MIKE21 SW can be used to calculate the wave conditions and associated radiation stresses.

Basic Equations

The governing equations is the wave action balance formulated in either Cartesian or spherical coordinates. In horizontal Cartesian coordiantes, the conservation equation for wave action can be written as

$$\frac{\partial N}{\partial t} + \nabla \cdot (\vec{v} N) = \frac{S}{\sigma} \qquad (4.1)$$

where N is the action density, t is the time, $\vec{v}$ is the propagation velocity of a wave group in the four dimensional phase space and S is the source term for energy balance equation. ∇ is the four-dimensional differential operator in space. The energy source term, S, represents the superposition of source functions describing various physical phenomena

$$S = S_{in} + S_{nl} + S_{ds} + S_{bot} + S_{surf} \quad (4.2)$$

S_{in} represents the generation of energy by wind, S_{nl} is the wave energy transfer due non-linear wave-wave interaction, S_{ds} is the dissipation of wave energy due to whitecapping, S_{bot} is the dissipation due to bottom and S_{surf} is the dissipation of wave energy due to depth-induced breaking.

Numerical Implementation

The discretization of the governing equation in geographical and spectral space is performed using cell-centered finite volume method. In the geographical domain, an unstructured mesh technique is used. The time integration is performed using a fractional step approach where a multi-sequence explicit method is applied for the propagation of wave action.

Ouput Data

The following types of output data is possible

- Parameters
  - Integral wave parameters
  - Input parameters
  - Model parameters
- Spectral parameter (directional spectrum): The direction energy/ action spectrum is obtained by integration over the discretised frequencies.
- Spectral parameter (frequency spectrum): The direction energy/ action spectrum is obtained by integration over the discretised directions.
- Spectral parameter (directional-frequency spectrum): The direction energy/ action spectrum is obtained by integration over the discretised frequencies.

4.2.2. MIKE21 Flexible Mesh - HydroDynamic Model

MIKE 21 Flow Model FM is a new modelling system based on a flexible mesh approach. The modelling system has been developed for applications within oceanographic, coastal and estuarine environments.

MIKE 21 Flow Model FM is composed of following modules:

- Hydrodynamic Module
- Transport Module
- ECO Lab/Oil Spill Module
- Particle Tracking Module
- Mud Transport Module
- Sand Transport Module

The Hydrodynamic Module is the basic computational component of the entire MIKE 21 Flow Model FM modelling system providing the hydrodynamic basis for the Transport Module, ECO Lab/Oil Spill Module, Mud Transport Module, Particle Tracking Module and Sand Transport Module.

The Hydrodynamic Module is based on the numerical solution of the two dimensional shallow water equations - the depth-integrated incompressible Reynolds averaged Navier-Stokes equations. Thus, the model consists of continuity, momentum, temperature, salinity and density equations. In the horizontal domain both Cartesian and spherical coordinates can be used.

The local continuity equation is written as

$$\frac{\partial u}{\partial x}+\frac{\partial v}{\partial y}+\frac{\partial w}{\partial z}=S \tag{4.3}$$

and the two horizontal momentum equations for the x- and y- component, respectively

$$\frac{\partial u}{\partial t}+\frac{\partial u^2}{\partial x}+\frac{\partial vu}{\partial y}+\frac{\partial wu}{\partial z}=fv-g\frac{\partial \eta}{\partial x}-\frac{1}{\rho_o}\frac{\partial p_a}{\partial x}-\frac{g}{\rho_o}\int_z^\eta \frac{\partial \rho}{\partial x}dz-\frac{1}{\rho_o h}\left(\frac{\partial s_{xx}}{\partial x}+\frac{\partial s_{xy}}{\partial y}\right)+F_u+\frac{\partial}{\partial x}\left(v_t\frac{\partial u}{\partial z}\right)+u_sS \tag{4.4a}$$

$$\frac{\partial v}{\partial t}+\frac{\partial v^2}{\partial y}+\frac{\partial uv}{\partial x}+\frac{\partial wv}{\partial z}=-fu-g\frac{\partial \eta}{\partial y}-\frac{1}{\rho_o}\frac{\partial p_a}{\partial y}-\frac{g}{\rho_o}\int_z^\eta \frac{\partial \rho}{\partial y}dz-\frac{1}{\rho_o h}\left(\frac{\partial s_{yx}}{\partial x}+\frac{\partial s_{yy}}{\partial y}\right)+F_v+\frac{\partial}{\partial z}\left(v_t\frac{\partial v}{\partial z}\right)+v_sS \tag{4.4b}$$

Where t is the time; x, y, z are the Cartesian coordinates; η is the surface elevation; d is the still water depth; $h=\eta+d$ is the total water depth; u, v, w are the velocity components; f is the Coriolis parameter; g is the gravitational acceleration; ρ is the water density; s_{yx} components of radiation stress tensor; ρ_o is the reference water density; S is the magnitude of the discharge due to point sources and (u_s, v_s) is the velocity by which the water is discharge into the ambient water; F_u, F_v are the horizontal stress terms.

The spatial discretization of the primitive equations is performed using a cell centered finite volume method. The spatial domain is discretized by subdivision of the continuum into non-overlapping element/cells. In the horizontal plane an unstructured grid is used comprising of triangles or quadrilateral element. An approximate Riemann solver is used for computation of the convective fluxes, which makes it possible to handle discontinuous solutions.

For the time integration an explicit scheme is used.

The application areas generally involve problems where flow and transport phenomena are important with emphasis on coastal and marine applications, where the flexibility inherited in the unstructured meshes can be utilized.

4.2.3. MIKE21 Flexible Mesh - Sediment Transport Model

It is a module for calculating non-cohesive sediment transport rates. You can calculate sand transport based on pure current information, or you can take waves into consideration too. In addition to sand transport rates, a simulation will give you the initial rates of bed level changes. This is sufficient to identify potential areas of erosion or deposition, but can not take the place of a full morphological model. It can be applied in tidal inlets, estuaries, coast lines and man made constructions like harbours and bridges. Tide, wind wave and current can all be taken into consideration for optimum precision in the simulations.

4.2.4. MIKE21/3 Coupled Model FM

MIKE 21/3 Coupled Model FM is a truly dynamic modelling system for applications within coastal, estuarine and river environments. MIKE 21/3 Coupled Model FM is composed of following modules:

- Hydrodynamic Module
- Transport Module
- ECO Lab / Oil Spill Module
- Mud Transport Module
- Particle Tracking Module
- Sand Transport Module
- Spectral Wave Module

The Hydrodynamic Module and the Spectral Wave Module are the basic computational components of the MIKE 21/3 Coupled Model FM. Using MIKE 21/3 Coupled Model FM it is possible to simulate the mutual interaction between waves and currents using a dynamic coupling between the Hydrodynamic Module and the Spectral Wave Module. The MIKE 21/3 Coupled Model FM also includes a dynamic coupling between the Mud Transport Module and the Sand Transport Module and the Hydrodynamic Module and the Spectral Wave Module. Hence, a full feedback of the bed level changes on the waves and flow calculations can be included.

The Hydrodynamic Module simulates water level variations and flows in response to a variety of forcing functions in lakes, rivers, estuaries and coastal regions. The effects and facilities include

- Flooding and drying
- Momentum dispersion
- Bottom shear stress
- Coriolis force
- Wind shear stress
- Barometric pressure gradients
- Ice coverage
- Tidal potential
- Precipitation/evaporation

- Wave radiation stresses
- Sources and sinks

The Hydrodynamic Module can be used to solve both three-dimensional (3D) and two-dimensional (2D) problems. In 3D the model is based on the numerical solution of the three-dimensional incompressible Reynolds averaged Navier-Stokes equations invoking the assumptions of Boussinesq and of hydrostatic pressure. Thus, the model consists of continuity, momentum, temperature, salinity and density equations and is closed by a turbulent closure scheme. In 2D the model is based on the shallow water equations – the depth-integrated incompressible Reynolds averaged Navier-Stokes equations.

The application areas are generally problems where flow and transport phenomena are important with emphasis on river, coastal and marine applications, where the flexibility inherited in the unstructured meshes can be utilized.

MIKE 21/3 Coupled Model FM can be used for investigating the morphological evolution of the nearshore bathymetry due to the impact of engineering works (coastal structures, dredging works etc.). The engineering works may include breakwaters (surface-piercing and submerged), groins, shoreface nourishment, harbours etc. MIKE 21/3 Coupled Model FM can also be used to study the morphological evolution of tidal inlets.
It is most suitable for medium-term morphological investigations (several weeks to months) over a limited coastal area. The typical dimensions are about 10 km in the alongshore direction and 2 km in the offshore direction. The computational effort can become quite large for long-term simulations, or for larger areas

5. INVESTIGATION OF THE SEDIMENT TRANSPORT TRENDS FOR THE EXISTING SITUATION (DN SCENARIO).

The first scenario investigated is the existing port layout, without any expansion works, along with the current morphology of adjacent coastlines. This case refers to as the "**Do Nothing**" scenario (**DN** hereafter).

As mentioned in Chapter 2, the port is protected by two breakwaters, the southern (windward) and the eastern (leeward). The port entrance is orientated eastwards (see Figure 2-2). There are two main quays, the northern of 360m length and the western of 125m. It has a turning circle of 280m diameter, and the water depth is about 9m. The **DN** layout is depicted in the following figure.

Figure 5-1. Existing port layout and current shoreline morphology - Do Nothing scenario.

5.1. Input Data

Under the framework of the present study, the consultants were provided with topographic and bathymetric surveys in the area of Vassilikos, by the Department of Lands and Surveys. Topographic and Bathymetric data, with a spatial resolution of 10m, extracted from the Digital Terrain Model (DTM) of the area, were obtained which for the purpose of this study are considered fully adequate.

The specific data are used for construction of flexible meshes representing the sea bottom along the coastal area. The bathymetric mesh **BATH_ DN and BATH_DN_MESH** (see Appendix) was constructed, covering an area of approximately 7.0km x 2.0 km, with 33.626 nodes and 65.393 elements.

The wave input data are presented in Table 3-5 consisting of ten (10) wave conditions.

5.2. Numerical Simulation of Nearshore Wave Propagation with MIKE21 SW Model for DN Layout

Figures with a SW prefix represent the output of the Spectral SW module of MIKE 21.
Figures for each incoming wave case were produced, depicting the wave height distribution all over the examined area (e.g., SW_S_DN_1, see **Appendix)**.. Figures with a suffix DN_1 (e.g., SW_S_DN_1) illustrate the wave field generated using as a boundary condition the highest wave characteristics per direction, whereas Figures with a suffix DN_2 (e.g., SW_S_DN_2) illustrate the wave field generated using as a boundary condition the equivalent wave characteristics per direction.

General observations and comments on the results:

- The coastal front in the area of interest is mainly susceptible to waves coming from the SSW, WSW, S, SSE and ESE. The highest and most frequently occuring waves are incident from SSW and WSW direction with an annual frequency of occurrence of 52.65% and 33.88% respectively. Waves from the S, ESE and SSE directions are less dominant with an annual frequency of occurrence of 4.56%, 2% and 1.58% respectively.
- As waves approach the shoreline, the wave heights are decreasing due to depth-induced wave breaking. The wave direction tends to be perpendicular to the shoreline due to refraction effects.
- The width of the breaking zone varies depending on the incoming wave characteristics (height and wave angle of incidence). For example, for waves travelling from SSW and incoming wave height Hs = 4,50m, the breaking zone starts approximately 400m away from the shoreline, while for waves travelling from SSE and incoming wave height Hs = 2,50m, the breaking zone starts at approximately 300m away from the shoreline.

5.3. Numerical Simulation of Nearshore Hydrodynamic Field with MIKE21 FM-HD Model for DN Layout

Figures with a HD prefix represent the output of the Hydrodynamic HD module of MIKE 21.

Figures for each incoming wave case were produced, depicting the current speed distribution all over the examined area (e.g., HD_S_DN_1, see **Appendix)**.
Figures with a suffix DN_1 (e.g., HD_S_DN_1) illustrate the current speed field generated using as a boundary condition the highest wave characteristics per direction whereas Figures with a suffix DN_2 (e.g., HD_S_DN_2) illustrate the current speed field generated using as a boundary condition the equivalent wave per direction.

General observations and comments on the results:

- In general wave-induced longshore currents are parallel to the shoreline decaying rapidly seaward of the breakers. These currents are generated by gradients in momentum flux (radiation stress) due to the decay of obliquely incident waves.

- Wave-induced currents of significant speed are evident at either side of the port predominantly due to waves coming from the SSW (210^0) and WSW (240^0) sectors.
- Waves incident from **South direction**, generate two main currents with opposite directions. The first one, west of the port, travels alongshore, from the edge of the windward breakwater to the west boundary of the study area. The second one, on the east side of the port has an opposite direction (eastward). In addition, an eddy is formed right eastward of the existing leeward breakwater. The depth-averaged current velocities on the west side reach values up to 0.8m/sec nearshore. At the east side of the port the equivalent currents are approximately of the same magnitude. These current values correspond to incident wave height, Hs, of 2.0m
- Waves incident from **SSW direction**, generate strong currents with general direction from West to East. The current velocities on the east side reach values up to 1.4m/sec. At the west side of the port the currents are weaker with magnitudes which reach 1.0m/sec. Again, an eddy is formed starting from the tip of the windward breakwater heading towards the root of the existing leeward breakwater.
- Waves propagating from **WSW direction**, generate currents with general direction from West to East. The current velocities in the east side are up to 0.9m/sec. At the west side of the port the currents reach magnitudes up to 0.7m/sec.
- Waves propagating from **SSE direction**, generate currents with general direction from East to West. The current velocities in the east side are up to 0.9m/sec. At the west side of the port, they reach 1.0m/sec.
- Waves incident from **ESE direction**, also generate currents with general direction from East to West. The current velocities in the east side are up to 0.9m/sec and in the west side of the port the currents are up to 1.0m/sec.

5.4. Numerical Simulation of Nearshore Sediment Transport Field with MIKE21 FM-ST Model for DN Layout

Figures with a ST prefix represent the output of the Sediment Transport ST module of MIKE 21.

Figures for each incoming wave case were produced, depicting the rate of bed level change distribution all over the examined area (e.g., ST_S_DN_1, see **Appendix)**. Figures with a suffix DN_1 (e.g., ST_S_DN_1) illustrate the rate of bed level change field generated using as a boundary condition the highest wave characteristics per direction whereas Figures with a suffix DN_2 (e.g., ST_S_DN_2) illustrate the rate of bed level change field generated using as a boundary condition the equivalent wave per direction.

It is well known and widely accepted that the sediment transport direction follows in general the respective longshore current pattern for large wave heights, which is evident in the specific results.

Variable trends of accretion and erosion along the east coast are observed

Overall, accretive tendencies are evident at the windward side of the existing structures. Accretive patterns are also observed along the area west of the existing windward breakwater though this is a non-erodable area due to the existence of a coastal revetment. Alternating accretive and erosive trends are apparent along the coastline east of the port.

5.5. Integration of Storm Events per Year – Mean Annual Rate of Bed Level Change for DN Layout

An integration of all simulated events has been carried out, in order to determine the mean annual rate of bed level change in the area of interest. As weighting factor per wave event, the mean annual occurrence frequencies are adopted, which are given in Table 3-4. Figure **INT_DN** shows the weighted annual rate of sea bottom change.

It is observed that the dominant tendencies arising from the annual integration of all events are similar to those resulting from South-Southwest Waves. This was expected, since this is the predominant wave direction with a mean annual probability of occurrence of about 53% and it is also associated with the highest wave heights. Furthermore, currents generated by the breaking of obliquely incident waves generally dominate in and near the surf zone.

Variable trends of accretion and erosion along the east coast are observed. At the west side of the port and more specifically at the root of the windward breakwater, an accretion and an erosion area are depicted.

6. GENERAL LAYOUT OF PROPOSED WORKS – Wl1

The General Layout **W1**, as optimized by the wave penetration study using numerical modeling, is investigated herein, from a coastal impact standpoint, using again numerical modeling. More specifically, the following proposed works are taken into account:

- Removal of the last 400m of the existing windward breakwater and 1240m extension
- Construction of a new 275m long leeward breakwater
- Construction of a 230m long x 125m wide pier at the location of the existing leeward breakwater
- Extension of coastal quay westward of the existing port basin 115m long / -9m deep.
- Extension of the quay to the north of the existing port basin 50m long / -9m deep
- Construction of a new quaywall north of the new port basin 385m long / -15m deep.
- Construction of a new quaywall east of the new port basin 195m long /-15m deep.
- Construction of a new quaywall along the inner side of the windward breakwater 1035m long / variable depth between -9m, -13m and -15m.
- Dredging of the new port basin at -15m CD
- Dredging the area between the new and the existing port basin at -13m CD
- Dredging of the new entrance channel at -16.5m CD

Layout W1 is shown in Figure 6-1.

Figure 6-1. Proposed layout - W1 scenario.

7. NUMERICAL SIMULATION FOR THE PROPOSED LAYOUT

The second scenario investigated is **W1** port layout (as described in the previous Chapter).

7.1. Input Data

As mentioned above, the consultants were provided with topographic and bathymetric surveys in the area of Vassilikos, and in conjunction with drawings of W1 layout, a flexible mesh was created representing the coastline and the sea bottom. The bathymetric mesh **BATH_W1 and BATH_W1_MESH** (see Appendix) was constructed, covering exactly the same area as for layout DN (approximately 7.0km x 2.0 km), with 38.141nodes and 74.209 elements.

The wave input data are presented in Table 3-5 consisting of ten (10) wave conditions.

7.2. Numerical Simulation of Nearshore Wave Propagation with MIKE21 SW Model for DN Layout

Figures with a SW prefix represent the output of the Spectral SW module of MIKE 21.
Figures for each incoming wave case were produced, depicting the wave height distribution all over the examined area (e.g., SW_S_W1_1, see **Appendix)**. Figures with a suffix W1_1 (e.g., SW_S_W1_1) illustrate the wave field generated using as a boundary condition the highest wave characteristics per direction whereas Figures with a suffix W1_2 (e.g., SW_S_W1_2) illustrate the wave field generated using as a boundary condition the equivalent wave per direction.

General observations and comments in comparison with DN layout:

- A general observation, arising from comparison of the two alternatives, is that the port expansion works affect the nearshore wave field mainly very close to the port area.
- The extension of the windward breakwater provides a significant protection to the coastline east of the new lee breakwater for waves arriving from WSW, SSW and S directions.

7.3. Numerical Simulation of Nearshore Hydrodynamic Field with MIKE21 FM-HD Model for DN Layout

Figures with a HD prefix represent the output of the Hydrodynamic HD module of MIKE 21.
Figures for each incoming wave case were produced, depicting the current speed distribution all over the examined area (e.g., HD_S_W1_1, see **Appendix)**. Figures with a suffix W1_1 (e.g., HD_S_W1_1) illustrate the current speed field generated using as a boundary condition the highest wave characteristics per direction whereas Figures with a suffix DN_2 (e.g., HD_S_W1_2) illustrate the current speed field generated using as a boundary condition the equivalent wave per direction.

General observations and comments in comparison with DN layout:

- Waves incident from **South direction** generate two main currents with opposite directions as in DN layout. The first one, west of the port, travels alongshore, from the edge of the windward breakwater to the west boundary of the study area. The second has an opposite direction (eastward). The order of magnitude of velocities remains similar.
- Waves propagating from **SSW direction** generate strong currents with general direction from West to East at the east side of the port as in DN layout. However, attention must be paid in the resulting values of current velocity. The extension of windward breakwater along with the deepening of sea bottom (entrance channel), seem to affect positively the adjacent eastern coastal area and reduce the velocities, developing in this area, from 1.50m/sec to 0.90m/sec. Furthermore, in the shadow area of windward breakwater (east side of leeward breakwater) the velocities drop below 0.80m/sec, thus eliminating strong currents. Since the direction SSW is the predominant (most occurring with highest waves), this result will play a major role on the overall (annually integrated) sediment transport field in the vicinity of the port.
- As in the previous case, waves propagating from **WSW direction**, in interaction with proposed works of layout **W1**, generate currents at the east side of the port with significantly lower velocity values. For instance, in case of DN layout the velocities reach values up to 1m/sec while in W1 layout velocities remain lower than 0.75m/sec.
- Waves propagating from **SSE, ESE direction**, generate currents with general direction from East to West at the east side of the port, as in DN layout.

7.4. Numerical Simulation of Nearshore Sediment Transport Field with MIKE21 FM-ST Model for DN Layout

Figures with a ST prefix represent the output of the Sediment Transport ST module of MIKE 21.
Figures for each incoming wave case were produced, depicting the rate of bed level change distribution all over the examined area (e.g., ST_S_W1_1, see **Appendix)**. Figures with a suffix DN_1 (e.g., ST_S_W1_1) illustrate the rate of bed level change field generated using as a boundary condition the highest wave characteristics per direction whereas Figures with a suffix W1_2 (e.g., ST_S_W1_2) illustrate the rate of bed level change field generated using as a boundary condition the equivalent wave per direction.

The sediment transport pattern follows in general the respective water flow pattern as described above. Variable trends of accretion and erosion along the east coast are observed.

7.5. Integration of Storm Events per Year – Mean Annual Rate of Bed Level Change for DN Layout

An integration of all simulated events has been carried out, in order to determine the mean annual rate of bed level change in the area of interest. As weighting factor per wave event, the mean annual occurrence frequencies are adopted, which are given in Table 3.7. Figure **INT_W1** shows the weighted annual rate of sea bottom change.

Once again it is observed that the dominant tendencies arising from the annual integration of all events are similar to those resulting from South-Southwest Waves. Variable trends of accretion and erosion along the east coast are observed. At the west side of the port and more specifically at the root of the windward breakwater, an accretion and an erosion area are depicted.

In comparison with DN layout, it is observed that on the western side of the port, the accretive pattern is more prominent.

At the east side of the port, only a specific coastal zone is influenced significantly. This zone starts from the root of the new leeward breakwater and extends for 600m eastward (see Figure 7-1). Beyond this length, the resulting image of bed level change becomes similar to the respective of DN's, indicating that the proposed works will not affect either positively or negatively the sediment transport diet there.

Furthermore, it has to be mentioned that in the influence zone (of 600m), there is no evidence of strong sediment movement trends. The overall trend is to have calmer areas, with reduced sediment loss (blue colour in sea bed level changes) and consequently the existing tendencies in coastline changes will not be adversely affected. In addition, it is noted that the area consists mainly of rocky formations and coarse materials.

Based on the above results, it is concluded that the extension of the port will not affect adversely the coastline evolution either on the west or east side of the existing port.

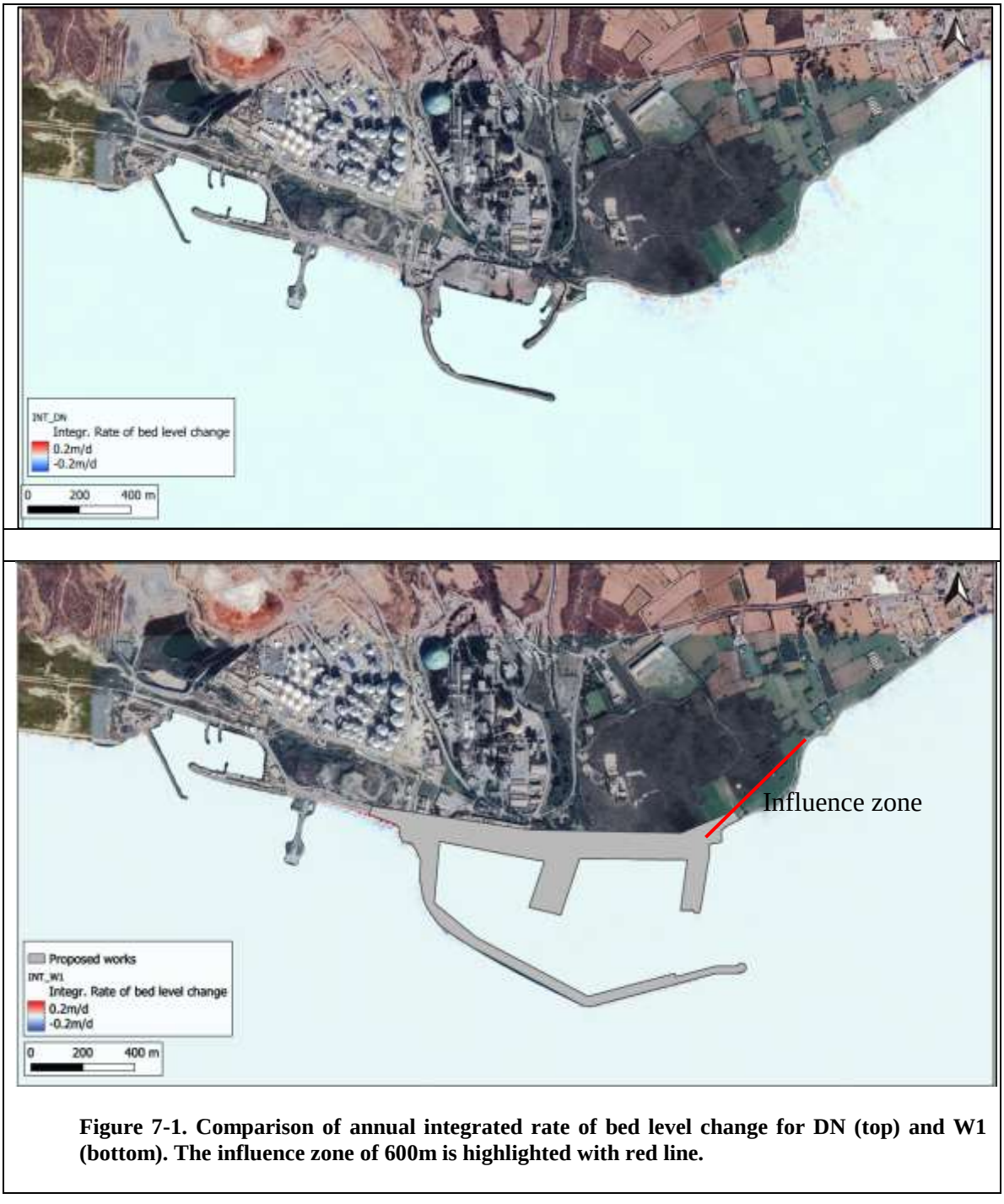

Figure 7-1. Comparison of annual integrated rate of bed level change for DN (top) and W1 (bottom). The influence zone of 600m is highlighted with red line.

8. CONCLUSIONS

The basic conclusions reached from the investigation on the **DN** alternative (current situation, without any port expansion works) are as follows:

- An inspection of historical trends of beach change has revealed various erosion areas at the coast east of the Port through the last decades.
- The predominant tendencies arising from the annual integration of all events are similar to those resulting from South-Southwest Waves.
- Variable trends of accretion and erosion along the east coast are observed

The basic conclusions that can be drawn from the investigation of the proposed works **W1** are summarized as follows:

- The extension of the windward breakwater offers a significant protection to the area east of the port for waves incident from WSW, SSW and S directions
- Once again it is observed that the predominant tendencies arising from the annual integration of all events are similar to those resulting from South-Southwest Waves. At the coast west of the port and more specifically at the root of the windward breakwater, accretive tendencies are intensified compared to the DN Scenario.
- At the east side of the port, the area affected by the works extends from the root of the new lee breakwater to about 600m towards the east. The overall trend in the influence area is to have calmer areas, with reduced sediment loss and consequently the existing tendencies in coastline changes will not be adversely affected.

The overall conclusion is that the expansion of the port will not adversely affect the coastal geomorphology on the eastern side of the existing port, while the slightly increased deposition trends observed in the west of the port, compared to the existing situation, are not deemed significant and as such they do not necessitate mitigation measures.